*Indian J Phys (September 2023) 97(10):2909–2915*
https://doi.org/10.1007/s12648-023-02628-9

ORIGINAL PAPER

# Structure and crystallization behavior of binary silver tellurite glasses and glass ceramics

**W Al-Mohammedi[1], M Sherbiny[1], A M Abdelghany[2] and G El-Damrawi[3]***

[1]Faculty of Science, Physics Departmental Al Azar University, Cairo 11651, Egypt

[2]Spectroscopy Department, Physics Research Institute, National Research Centre, Giza 12622, Egypt

[3]Glass Research Group, Physics Department, Faculty of Science, Mansoura University, Mansoura 35516, Egypt

Received: 29 April 2022 / Accepted: 06 February 2023 / Published online: 13 March 2023

**Abstract:** Using Raman spectroscopy in conjunction with X-ray diffraction (XRD), transmission electron micrographs (TEM-EDP), and scanning electron microscopy (SEM), the local environment of Te atoms and the crystallization behavior of glasses in the system of chemical formula $x\mathrm{Ag_2O}$. $(100 - x)\mathrm{TeO_2}$ $(25 \leq x \leq 50$ mol%) have been examined. Crystalline structure was evident in the XRD spectra of glasses containing 40 and 50 mol% $\mathrm{TeO_2}$. On the other hand, an amorphous structure has been observed in glasses with lower $\mathrm{Ag_2O}$ concentrations (25, 30, and 35 mol%). Thermal heating could be used to crystallize the amorphous glasses' structure. Using DSC measurements, the treatment's temperature was controlled. The species with good crystallinity include $\mathrm{Ag_2Te_4O_9}$ and $\mathrm{Ag_2Te_2O_5}$. The results of TEM and EDP, as well as both SEM and XRD, revealed that in glasses enriched with $\mathrm{Ag_2O}$, crystalline clustered species were formed. Raman data proved that the crystalline clustered is improved as a result of the formation of $\mathrm{TeO_3}$ units enriched with nonbridging oxygen bonds. In compositions containing less than 40 mol%, $\mathrm{Ag_2O}$ plays the role of a glass modifier. At higher $\mathrm{Ag_2O}$ concentrations, it plays the role of building crystalline clusters of the $\mathrm{Ag_2Te_4O_9}$ and $\mathrm{Ag_2Te_2O_5}$ types.

**Keywords:** Thermal treatment; Structural investigations; Telluride network; Glasses; Glass–ceramics

## 1. Introduction

Due to its possible use in optical devices, tellurite glasses have attracted a lot of research [1–7]. They exhibit high refractive indices and dielectric constants as well as good nonlinear optical transmittance [8–12]. Several structural studies on binary alkali tellurite glasses have been performed [5–9] using a range of structural techniques. Because the tellurium–oxygen polyhedron is so variable, it is difficult to predict how the structural environment distribution changes when the glass composition changes.

The notation $Q^n{}_m$ has been proposed for modified telluride glasses [13–17], where n signifies the amount of bridging oxygen (BO), and m determines the coordination number. Because the abundance of each tellurite polyhedron was supposed to be dependent on the species' charge, the number of non-charged tellurite polyhedra ($Q^4{}_4$) was thought to decrease as modifier oxide concentration increased. Alternatively, an increase in charged polyhedral ($Q^3{}_4$; $Q^1{}_3$, $Q^0{}_3$) units was simply observed.

The tellurium structural unit with the greatest $\mathrm{TeO_2}$ concentration and lowest modifier oxide is a four-coordinated trigonal-bipyramid $\mathrm{TeO_4}$ ($Q^4{}_4$), which may be generated in the paratellurite ($\alpha$-$\mathrm{TeO_2}$) polymorph of crystalline $\mathrm{TeO_2}$. Some of the stretched bonds can simple be broken when the $\mathrm{TeO_2}$ concentration was lowered, resulting in a three-coordinated structure known as ($Q^3{}_4$; $Q^1{}_3$; $Q^0{}_3$). A similar approach was considered in alkali-tellurite glass structures [15–17]. It was assumed that five tellurium polyhedra can be identified in tellurium glass systems modified by some extent of alkali or silver oxides [13–17].

Using $^{23}$Na NMR spectroscopy, the formation of crystalline clusters produced from $\mathrm{Na_2TeO_3}$ may then be validated [17]. Sodium ions appear to be randomly distributed at low concentrations. At intermediate concentrations, there is also a strong middle-range order. The existence of some crystalline phases in the sodium tellurite system has been confirmed. In sodium-rich glasses, however,

*Corresponding author, E-mail: gomaaeldamrawi@gmail.com

$Na_4Te_4O_{10}$ [13, 17, 18] and $Na_2TeO_3$ may form. Recent studies have shown that $Ag_2O$ plays a similar role as played by $Na_2O$ in $TeO_2$ glasses since $Ag_2TeO_3$ crystalline phases are confirmed to be formed in $Ag_2O$-rich glasses.

The objective of this work is to determine the impact of both glass composition and thermal heat treatment processes on the structure of tellurite glasses. The findings of XRD, TEM-EDP, and Raman spectroscopy of silver telluride glasses and their crystalline derivatives are presented in this study. The transformation of amorphous to crystalline silver tellurite phases gives the material an extra advantage to be used in the biomedical field of application. Additionally ordered tellurite glasses can be used as high refractive indices and dielectric constants materials.

## 2. Experimental details

### 2.1. Sample preparation

The melt quenching technique was used to prepare glasses in the system $x$$Ag_2O$. $(100 - x)TeO_2$, (25–50 mol%). Samples are obtained from reagent-grade mixtures of $AgNO_3$ and $TeO_2$ which have been melted in a Pt-Au crucible. To remove $NO_2$, the specimens were heat-treated at a slow rate of 2 °C/min from room temperature to 300 °C and then melted for 20–30 min between 700 and 800 °C before being quenched by pouring the melt between two metallic plates.

### 2.2. Sample characterization

A Shimadzu X-ray type Dx-30 diffractometer is used for X-ray diffraction measurements. The values of the maximum peak and intensity are used to determine the material type that is compared to patterns in the joint committee for powder diffraction 108 standards' international powder diffraction file (PDF) database (JCPDS). A transmission electron microscope (TEM) of type JEOL-JEM-1011 was used to determine the size and shape of the studied samples. Microstructural data were tested using the JSM-7500F field emission scanning electron microscope. The machine operated with an accelerated voltage of 25 kV. All samples were sputter-coated with a thin layer of gold (3–4 nm) to avoid sample charging and increase the signal-to-noise ratio. The samples containing 30 and 35 mol% $Ag_2O$ were heated in a muffle furnace (Heraeus KR170) with a temperature control of less than 2 °C. The samples were heat-treated at a temperature of 200 °C for a treatment time interval of 10 h. After heating, the glasses were then kept in the furnace and held at the temperature of heat treatment for the desired time before cooling normally at room temperature. Using a Raman confocal microscope, WITec model Alpha 300, with laser power of 532 nm, and 10 mw in the range of 200–2000 $cm^{-1}$ were recorded. The obtained spectra were deconvoluted to get information about the structural changes of the basic units in these glasses.

## 3. Results and discussion

### 3.1. XRD results

Depending on the glass composition, both crystalline and amorphous natures can be possessed in the studied binary silver tellurite glasses. Glasses containing 25, 30, and 35 mol% $Ag_2O$ have the amorphous structure which is the most dominant, as reflected from XRD patterns presented in Fig. 1. Higher $Ag_2O$ (40 and 50 mol%) concentration leads to the formation of a specific type of crystalline species in the main tellurite glass network.

As shown in Fig. 1, the tendency for crystal formation increases as the $Ag_2O$ content increases from 35 to 50 mol%. There are weak diffraction peaks visible in the spectra of glasses containing 35 and 40% mol%. Conversely, glasses with a higher $Ag_2O$ content can resolve XRD peaks that are more intense and sharp. The crystalline aggregate of Ag ions in the tellurite network is confirmed to be the source of two distinct diffraction peaks, specifically those at 33° and 38°. This behavior suggests that other silver-containing species may have developed in high silver-containing glasses.

Adding $Ag_2O$ at the expense of $TeO_2$ can directly convert $TeO_4$ to other units containing NBO atoms [15–17]. High modification levels, on the other hand, can

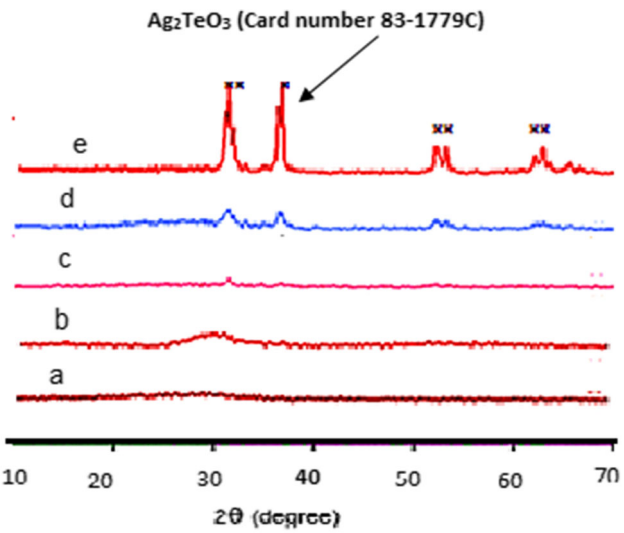


**Fig. 1** XRD spectra of glasses containing 25, 30, 35, 40, and 50 mol% $Ag_2O$, presented by (a), (b), (c), (d), and (e), respectively

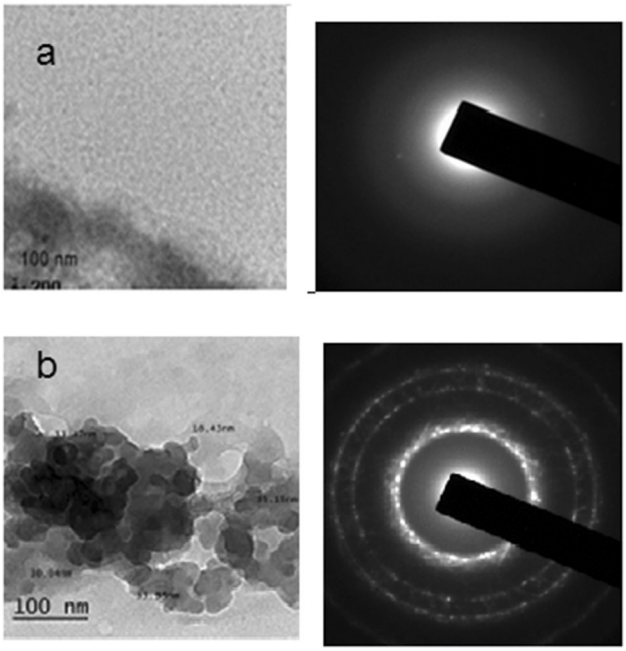


**Figures 2** (**a**, **b**), TEM images and the EDP of $TeO_2$ glass containing 30 and 50 mol% $Ag_2O$, respectively

result in the formation of more NBO as well as additional structurally clustered species in the telluride network. At extremely higher $Ag_2O$ content (40 and 50 mol%), as in the present study, most $Ag_2O$ can be consumed to build crystalline cluster species of type $Ag_2TeO_3$ [12–14]. This role was identified to be dependent on the bond type formed between Ag cation and oxygen ions. These findings suggest that at high $Ag_2O$ concentrations [13, 14], it would be difficult to confirm its modifier role only in the binary-modified glasses, but it can play an additional role that appears in cluster formation.

Based on the above arguments, it can be concluded that $TeO_4$ tetrahedral units are the main forming species in the telluride network. Some ordered $TeO_4$ groups can be converted to $TeO_3$ units after the addition of a modifier [12–19]. Extremely high modifier contents can result in extra $TeO_3$ groups. (The tellurium unit contains one and two nonbridging oxygen atoms.) Furthermore, some crystalline species of type $Ag_2TeO_3$ are formed in silver-rich telluride glasses as well as $Na_2TeO_3$ crystalline clusters which have been formed in silver and sodium-rich telluride glasses [14, 17, 19].

### 3.2. TEM-EDP results

Figure 2 presents the TEM micrograph with its electron diffraction pattern (EDP) for two different compassions (30 and 50 mol% $Ag_2O$) that were introduced as examples for the amorphous and crystallized samples, respectively. As shown in Figs. 2(a and b), the main structural groups are distributed separately with an irregular repetition. Furthermore, in the composition of higher $Ag_2O$ content (50 mol% $Ag_2O$), the specific types of clusters are seen to be distributed as aggregates or clusters in the host main network. The above arguments agree well with the general concept of cluster formation [8–11]. In such a situation, the term "cluster" is generally defined as an aggregate or accumulation of bound atoms or molecules that are between the sizes of a molecule and a bulk solid [8, 9]. This argument was supported to a great extent by experimental studies of Ag-rich telluride glasses, which revealed the presence of Ag clusters when the concentration of $Ag_2O$ is relatively high (50 mol% or more), see Fig. 2. In the sample of composition 50 mol% $Ag_2O$, the highly crystallized telluride and Ag metallic phases are the dominant phases.

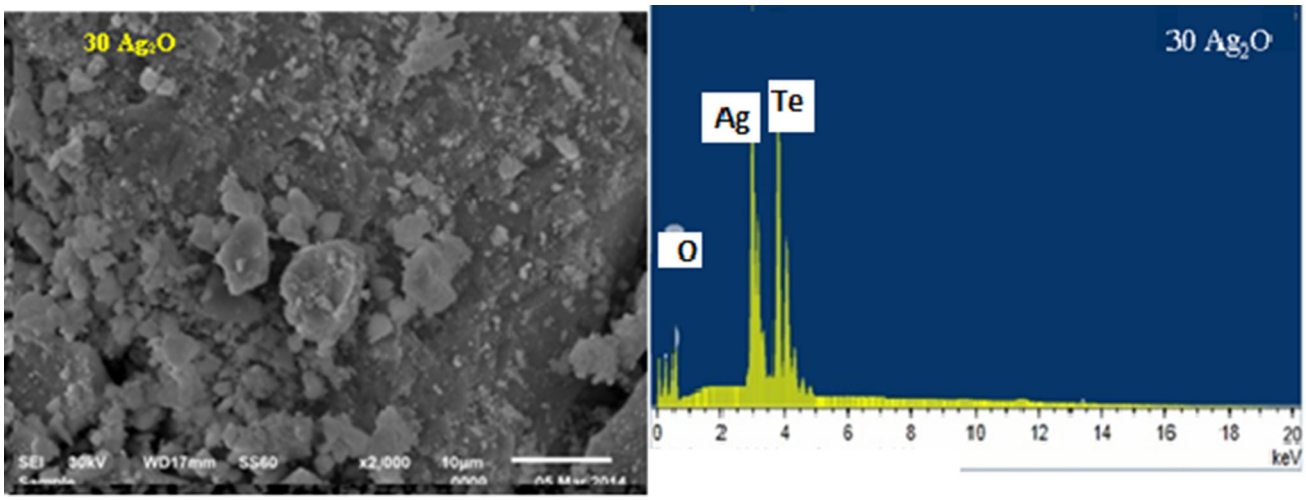


**Fig. 3** SEM micrographs and EDS spectrum glass of 30 mol% $Ag_2O$

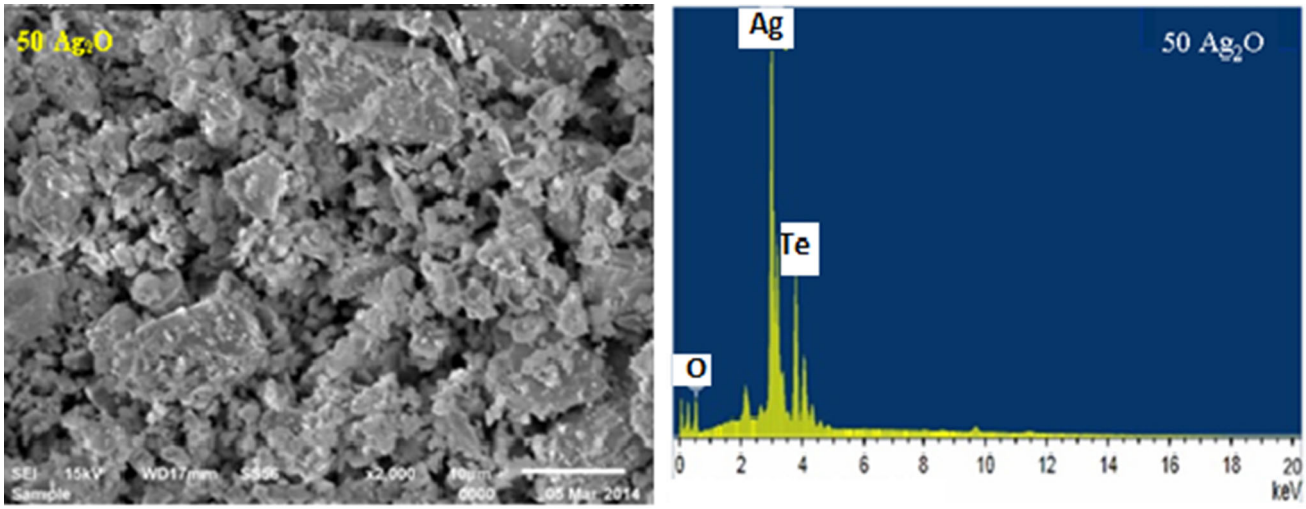


**Fig. 4** SEM micrographs and EDS spectrum glass of 50 mol% $Ag_2O$ TEM, EDP morphology, and phase analysis

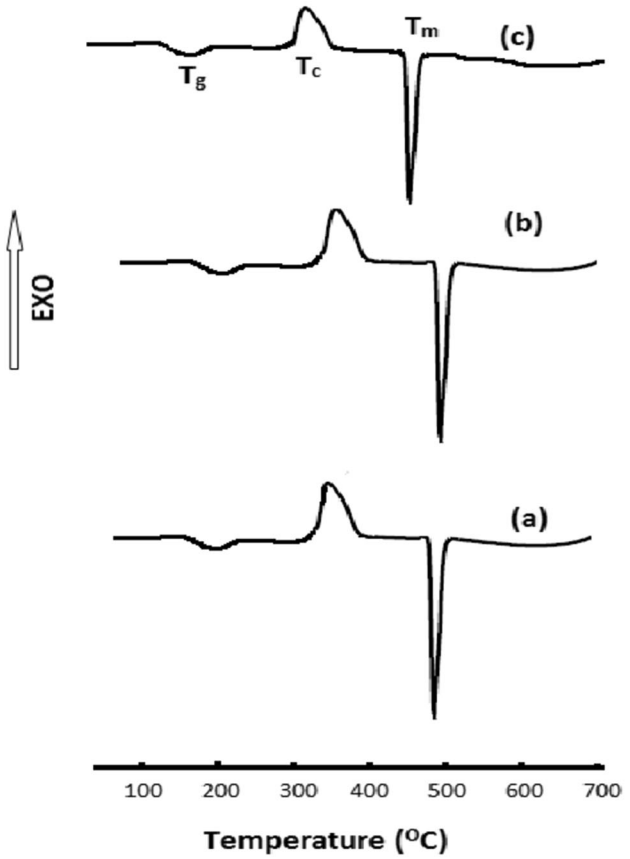


**Fig. 5** DSC curves for samples containing 25, 30, and 35 mol% $Ag_2O$(a, b, c), respectively

As a general conclusion, all of the investigated glasses of $Ag_2O/TeO_2 \geq 1$ are highly crystallized into homogeneous telluride and Ag metallic phases. But in samples of lower $Ag_2O/TeO_2$ molar ratio, on the other hand, a significant difference is considered. The formation of

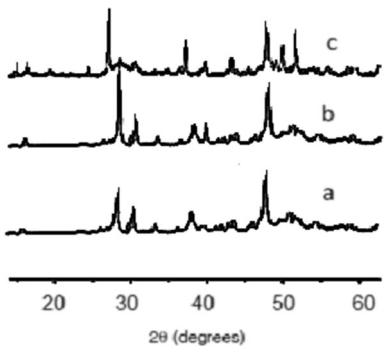


**Fig. 6** XRD spectra for the sample containing 25 (**a**), 35(**b**), and 40 mol% (**c**) $Ag_2O$ treated thermally at 200 °C for 10 h

crystalline clusters required more NBO and silver ions to be accumulated.

### 3.3. SEM–EDS spectra

On a selection of compositions, SEM–EDS analyses were performed to determine how composition affected morphology. Figures 3 and 4 display the SEM images and EDS spectra of glasses with 30 and 50 mol% $Ag_2O$, respectively. There are tellurium, oxygen, and silver peaks to be seen. With an increase in $Ag_2O$ content, Ag's silver peak intensity increases. The two peaks for Ag and Te atoms are virtually similar at 30 mol% $Ag_2O$, indicating that $Ag_2O$ is only used in $TeO_2$ modification. However, the sample with a 50 mol% Ag content had a higher peak intensity of Ag than Te. The XRD and TEM-EDP results are both confirming the higher level of modification of Ag to form accumulated crystalline clusters. As an alternative, it is also thought that the higher loading of Ag at the expense of Te atoms is the reason for the increase in relative intensity.

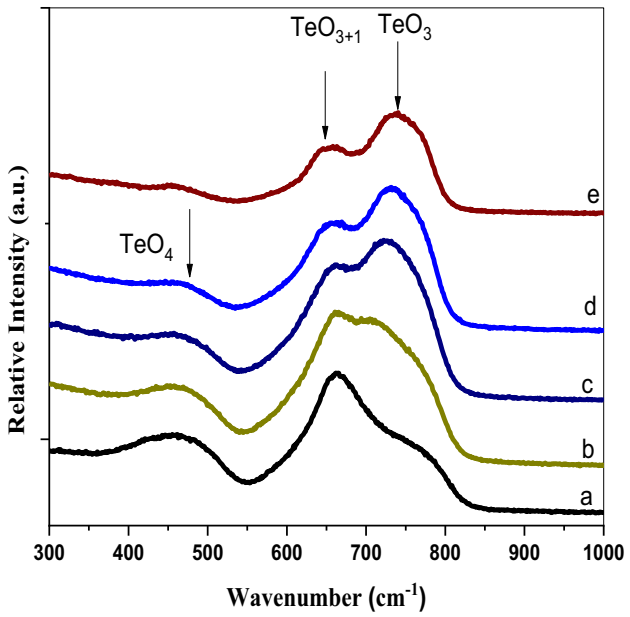


**Fig. 7** Raman spectra of glasses containing 25, 30, 35, 40, and 50 mol% $Ag_2O$

Then, SEM micrograph of the sample of 30 mol% $Ag_2O$ is different from that of the samples of 50 mol%. More overcrowded species were present in the morphology of glass enriched with $Ag_2O$, which could be combined to produce more intense shapes.

### 3.4. Effect of thermal heating

It can be realized from XRD patterns (Fig. 1) that samples of 25, 30, and 35 mol% $Ag_2O$ possessed an amorphous structure. Therefore, the thermal heat treatment at 200 °C provided by the DSC curves (Fig. 5) was shown to have a significant impact on the structure of the presented compositions. The amorphous structure of 25, 30, and 35 mol% $Ag_2O$-containing glasses could be changed into a more regular structure as seen from XRD spectra (Fig. 6) of samples treated thermally at 200 °C for 10 h. The pattern from untreated samples is compared with the XRD patterns in Fig. 6. At 200 °C, the sample is almost completely crystalline, with a little amount of glass phase visible in the background. The ordering of the Ag cations in the primary tellurite network is the polymorph of $Ag_2Te_4O_9$ [20–22]. This crystalline species is thought to be a metastable silver-like compound found in silver telluride samples with compositions of 30 and 35 mol% $Ag_2O$.

### 3.5. Raman spectra

Raman spectral data are a complementary measurement that may be used for the investigation of the vibrational modes of the molecules that relies upon inelastic scattering [23, 24].

It can be shown from Fig. 7 that both the intensity and relative area of the Raman bands at about (400–500 $cm^{-1}$) and 600–700 $cm^{-1}$) assigned to $TeO_4$ and $TeO_{3+1}$ showed a decreasing trend. Such smearing bands can be assured through the deconvolution analysis technique (DAT) previously discussed by different authors [25–29]. Figure 8 is an example of the deconvoluted spectra for two samples of glasses. The analyzed values of the relative area for each band are listed in Table 1. However, the band representing $TeO_3$ units (between 700 and 800 $cm^{-1}$) has shown an inverse trend which leads to the formation of NBO in $TeO_4$ units which is transformed into $TeO_3$ units via the formation of NBO atoms. The formation of NBO in the $TeO_2$ network at high $Ag_2O$ concentrations (40 and 50 mol%) is considered the main reason for the formation of crystalline clustered species detected by SEM and TEM micrographs.

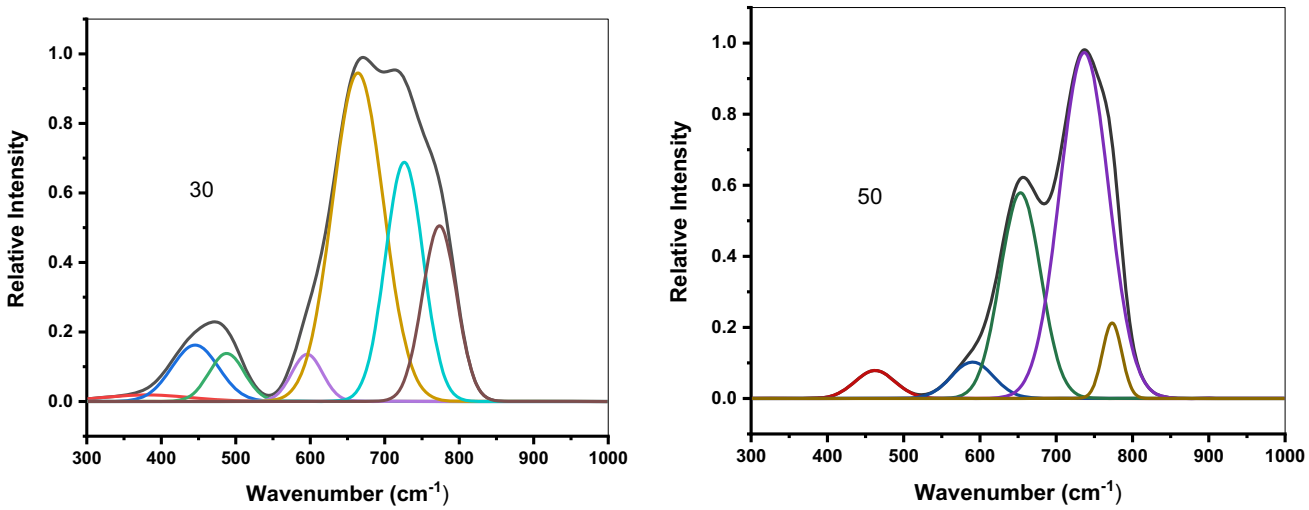


**Fig. 8** Raman deconvoluted spectra for the sample containing 30 and 50 mol%

**Table 1** Relative area for each component FTIR band

| $Ag_2O$ mol% | Relative area 400–500 $cm^{-1}$ | Relative area 600–700 $cm^{-1}$ | Relative area 700–800 $cm^{-1}$ |
|---|---|---|---|
| 25 | 0.24 | 0.42 | 0.34 |
| 30 | 0.22 | 0.36 | 0.42 |
| 35 | 0.16 | 0.31 | 0.53 |
| 40 | 0.11 | 0.25 | 0.54 |
| 50 | 0.07 | 0.20 | 0.63 |

## 4. Conclusions

The XRD spectra of glasses in the $xAg_2O.(100 - x)TeO_2$ ($25 \leq x \leq 50$ mol%) showed significant changes as the glass composition changed. XRD patterns have shown that some crystalline phases can be formed without thermal treatment. On the other hand, the amorphous glasses containing 25, 30, and 35 mol% $Ag_2O$ could be crystallized through a thermal heating process. The Raman spectra have specific features characterizing different telluride structural units. When the glass network becomes rich with $Ag_2O$ content, most of the available $TeO_4$ and $TeO_{3+1}$ units are transformed into $TeO_3^-$, $TeO_3^{2-}$, and Ag-Te species. The TEM and EDP data agree well with the XRD results, indicating the formation of crystalline clustered species in glasses enriched with $Ag_2O$.

**Author Contribution** GED suggests the object of study, interpreted the data and wrote early drafts of the manuscript. WAM performed in situ measurements including Raman and XRD spectroscopy. MS and AA conceptualized the experiment and revised the drafts and final version of the manuscript. All authors read and approved the final manuscript.

**Funding** Open access funding provided by The Science, Technology & Innovation Funding Authority (STDF) in cooperation with The Egyptian Knowledge Bank (EKB).

**Declarations**

**Conflict of interest** We declare that we have no financial and personal relationships with other people or organizations that can inappropriately influence our work, and there is no professional or other personal interest of any nature or kind in any product, service, or company that could be construed as influencing the position presented in or the review of, the manuscript entitled.



## References

[1] C Devaraja, G J Gowda and B Eraiah *K. Keshavamurthy Ceram. Inter.* **47** 7602 (2021)
[2] R El-Mallawany, W M Abou-Taleb, M A Naeem and M E Krar *Optik* **242** 167171 (2021)
[3] N Effendy, H A A Sidek, M K Halimah and M H M Zaid *Mater. Chem. Phys.* **273** 125156 (2021)
[4] A. Okasha, S.Y. Marzouk, A.M. Abdelghany *Opt. Laser Technol.* **137**106829 (2021)
[5] K.I. Hussein, A.M. Al-Syadi, M.S. Alqahtani, N. Elkhoshkhany, H. Algarni, M. Reben, E.S. Yousef *Materials* **15** 2403 (2022)
[6] S B Mallur and P K Babu *Mater. Res. Bull.* **147** 111651 (2022)
[7] M.S. Al-Buriahi, C. Eke, Z.A. Alrowaili, A.M. Al-Baradi, I. Kebaili, B.T. Tonguc *Optik* **249** 168257 (2022)
[8] R G Capelo, J M Almeida, D F Franco, G Y Poirier, C R Mendonça and M Nalin *D. Manzani J. Mater. Res. Technol.* **13** 1296 (2021)
[9] J de Clermont-Gallerande, S Saito, M Colas and P Thomas *J. Alloys Compd.* **854** 157072 (2021)
[10] R.P. Kumbhakar, S.K. Dhiman, S.K. Mahajan, G.F. Ansari *Mater. Today: Proc.* **56** 1313 (2022)
[11] S Suehara, P Thomas, A Mirgorodsky, T Merle-Méjean, J C Champarnaud-Mesjard and T Aizawa *J. Non-Cryst. Solids* **345** 730 (2004)
[12] E M Roginskii, V G Kuznetsov, M B Smirnov, O Noguera, J R Duclère and M Colas *J. Phys. Chem. C* **121** 12365 (2017)
[13] T Sekiya, N Mochida, A Ohtsuka and M Tonokawa *Journal of non-crystalline solids* **144** 128 (1992)
[14] J.C. McLaughlin, S.L. Tagg, J.W. Zwanziger *J. Phys. Chem. B* **105** 67 (2001)
[15] M Soulis, A P Mirgorodsky, T Merle-Méjean, O Masson and P Thomas *J. Non-Cryst. Solids* **354** 143 (2008)
[16] D. Souri, Z.E. Tahan, S.A. Salehizadeh *Indian J.Phys.* **90** 407 (2016)
[17] S Hashim and S K Ghoshal *Indian J. Phys.* **94** 1811 (2020)
[18] H Elkholy, H Othman, I Hager, M Ibrahim and D de Ligny *Materials* **12** 4140 (2019)
[19] P Sharma, D K Kanchan, M Pant and K P Singh *Mater. Sci. Appl.* **1** 59 (2010)
[20] B.V.R. Chowdari, P.P. Kumari *Solid State Ion.* **86** 521 (1996)
[21] D. Souri *Indian J.Phys.* **89** 1277 (2015)
[22] G El-Damrawi, A M Abdelghany, M I Abdelghany and M A Madshal *Materialia* **16** 101095 (2021)
[23] K. Sklepić, M. Vorokhta, P. Mošner, L. Koudelka, A. Mogus-Milankovic*J. Phys. Chem. B* **118** 12050 (2014)
[24] G El-Damrawi, H M Zahran and A M Abdelghany *J. Taibah Univ. Sci.* **15** 1123 (2021)

[25] A.M. Abdelghany, *Silicon*, **2** 179 (2010)
[26] A.M. Abdelghany & A. Behairy *J. Mater. Res. Technol.* **9** 10491 (2020)
[27] E I Kamitsos and G D Chryssikos *J. Mol. Struct.* **247** 1 (1991)
[28] A.G. Papadopoulos, N.S. Tagiara, E.D. Simandiras & E.I. Kamitsos *J. Phys. Chem. B* **124** 5746 (2020)
[29] N S Tagiara, D Palles, E D Simandiras, V Psycharis, A Kyritsis, E I Kamitsos and J Non-Cryst *Solids* **457** 116 (2017)